Research Article

Sandra Helena Messaddeq*, Antoine Dumont, Alexandre Douaud, Mohammed El-Amraoui and Younès Messaddeq

Formation of cross-superposed LIPSSs on bulk chalcogenide glasses using fs-laser

https://doi.org/10.1515/aot-2018-0031
Received June 13, 2018; accepted July 30, 2018; previously published online September 4, 2018

Abstract: This paper reports the formation of laser-induced periodic surface structures (LIPSS) observed on the ablated surface of bulk As_2S_3 chalcogenide glasses produced after irradiation by a focused beam of femtosecond Ti:sapphire (fs)-laser (1 kHz, 100 fs, 800 nm). By controlling the irradiation condition of fs-laser, high spatial frequency LIPSS (HSFL) ripples parallel to polarisation of the incident light are formed. Nanovoids with an average diameter of ~300 nm and depth of 200 nm also appear between the ripples. Furthermore, we show a transition from the HSFL features toward the formation of low-spatial-frequency LIPSS (LSFL) with an intermediated complex structure of ripples, which are oriented simultaneously parallel and perpendicular to the polarisation of the incident light that we call cross-superposed LIPSSs.

Keywords: chalcogenide; femtosecond; glass; laser; LIPSS.

1 Introduction

Chalcogenide glass materials (ChGs) have attracted significant interest not only because of their high refractive index (n = 2.6 at 0.6439 μm) and wide transparent window (up to 8 μm) depending on the glass composition and low phonon energy (350 cm^{-1}) [1] but also due to their high photosensitivity under illumination with continuous wave (CW) laser having photon energy comparable to the bandgap of the glass [2, 3]. In the field of photoinduced effects, the photosensitivity of As–S glasses has been widely studied during the last decades [4, 5] until nowadays [6, 7].

Contrary to the case of CW irradiation, when chalcogenide glass is exposed to infrared (IR) femtosecond (fs)-laser (1.55 eV), they become highly nonlinear, and this interaction results in permanent changes in the structure of the glass, which rely on multiphoton absorption [8]. One of the consequences of the exposure of bulk chalcogenide glasses to fs-laser pulses is the formation of laser-induced periodic surface structures (LIPSSs), namely, ripples. When the periodicity of the LIPSS is approximately equal to the wavelength of the incident light, it is usually termed low-spatial-frequency LIPSSs (LSFLs) [9].

A widely accepted model is that LIPSS, having a spatial period close to the irradiation wavelength $\Delta \cong \lambda$, results from interference of the incident beam with the surface-scattered waves originating from surface inhomogeneity [10–12]. The LIPSS orientation depends on the polarisation of the incident beam and the kind of material. For example, on metals and semiconductors (strong absorbing materials) the LIPSS are observed with an orientation perpendicular to the beam polarisation [13, 14], while in wide bandgap dielectrics, the LIPSSs often have an orientation parallel to the beam polarisation [15]. Nevertheless, it is also observed that ripples with both orientations perpendicular and parallel to the laser polarisation are formed on dense flint ZF_6 glass [16]. The authors propose that the formation of perpendicular ripples mainly resulted from the interference of an incident laser with a surface plasma wave, while the parallel ripples are formed by the Maragoni convection [17]. By studying the fs-laser ablation of a wide bandgap insulator (BaF_2), a complex structure of fine ripples was detected at the bottom of the ablated crater, which is oriented perpendicular to the beam polarisation, and a second, wider, periodic structure oriented parallel to the beam polarisation superimposed on the first

***Corresponding author: Sandra Helena Messaddeq,** Centre d'Optique, Photonique et Laser (COPL), Université Laval, Québec, Canada, e-mail: sandra.messaddeq@copl.ulaval.ca
Antoine Dumont, Alexandre Douaud, Mohammed El-Amraoui and Younès Messaddeq: Centre d'Optique, Photonique et Laser (COPL), Université Laval, Québec, Canada.
http://orcid.org/0000-0002-7642-8404 (A. Douaud)

one. Reif et al. [17] assume that the ripple structures are formed by self-organisation during the relaxation of the highly non-equilibrium surface after explosive positive ion emission.

The possibility of coexisting structures parallel and perpendicular to the polarisation of the incident light, namely cross-superposed LIPSSs, has been shown theoretically on the basis of the Sipe-Drude theory [18]. However, due to the lack of materials that exhibits such a complex structure, the cross-superposed LIPSSs have never been observed experimentally in chalcogenide bulk glasses.

In this paper, we present an observation of the LIPSS on bulk As_2S_3 chalcogenide glasses by ablation using femtosecond pulses. For the first time, we show the formation of cross-superposed LIPSSs oriented simultaneously perpendicular and parallel to the laser polarisation on bulk chalcogenide glasses. The period and depth of the structures were measured by atomic force microscopy (AFM) and scanning electron microscopy (SEM). The dependence of the morphology of the laser-induced periodic surface structures on the experimental parameters such as laser fluence, laser polarisation and irradiation time was investigated.

2 Experimental

Homogeneous bulk As_2S_3 glasses with optical quality were synthesised from (5N) elemental arsenic and sulphur (Sichuan Western Minmetals, Chengdu, Sichuan, China) and melted at 600°C in sealed silica ampoules in a rocking furnace for up to 12 h. The resulting rods were quenched in water and annealed near the glass transition temperature (180°C) during 6 h. The rods were subsequently sliced and polished so as to obtain 2-mm-thick samples.

A Ti-sapphire regenerative amplifier system [Coherent (Santa Clara, CA, USA) model Legend-HE] that produced pulses with a maximum energy of 3.5 mJ at a 1-kHz repetition rate with a central wavelength of 806 nm was used to expose the As_2S_3 samples. The temporal width of the Fourier-transform-limited pulses was measured to be ~34 fs, and the laser beam diameter was measured to be ~8.0 mm (at $1/e^2$) at the laser output. The beam was then focused using a 50-cm focal length plano-convex spherical lens. The samples were placed at a distance of 46 cm from the lens. The surface of the sample was positioned normal to the directional of the incident beam. Following irradiation, the surface morphologies of craters produced were analysed with a profilometer (DEKTAK/Bruker, Billerica, MA, USA), by SEM [FEI (Waltham, MA, USA) model Quanta 3D FEG] and by AFM (Veeco, Plainview, NY, USA).

3 Results and discussion

3.1 Ablation threshold and dependence on number of laser pulses – incubation effect

In order to determine the threshold energy changes under the action of fs-laser pulses, different number of pulses (N = 10–2000) were applied at different locations on the As_2S_3 surface at energies ranging from 0.1 to 2 mJ. The change in the surface topography is shown in Figure 1A. We observed that the action of the laser pulse induces craters on the surface of the glass. It is clear from the images that the ablated diameter increases with increasing shot number, thus, directly indicating an accumulation effect.

At a lower pulse number (N ≤ 100), the shape of the ablated region is very irregular due the intrinsic defects from the material. As ablation proceeds farther (N ≥ 1000), the craters become deeper and have a regular circular shape with a diameter similar to that of the laser beam (640 μm). We can note that at higher pulse number and

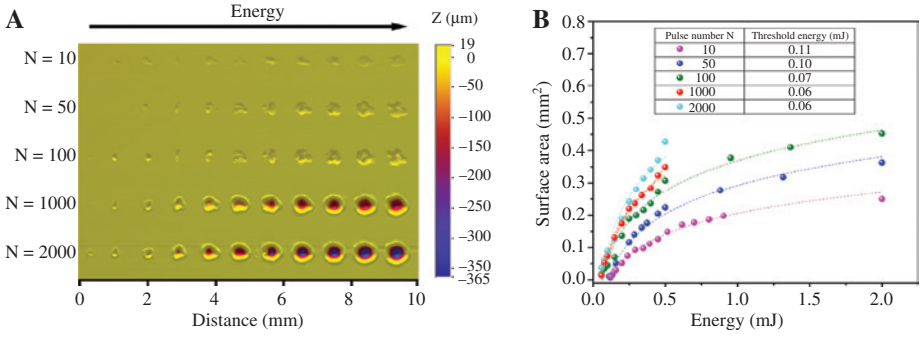

Figure 1: (A) AFM depth profile of the ablated areas, as a function of pulse number and energy. (B) Ablated area as a function of laser energy for different numbers of applied pulses on an As_2S_3 glass. The threshold energy is determined by the energy value when the fit goes down to A = 0.

low energy, a rim is formed at the edge of the crater, wherein the formation can be attributed to the fact that As_2S_3 is softer and has a lower melting point compared to fused silica where a rim was not observed [19].

As for determining the threshold energy value (E_{th}) for many pulses, we used the established procedure consisting of applying the 'zero damage method' [20] for various pulse superposition, including the single-pulse case. In this method, the surface of the sample is ablated at various energies by a Gaussian beam, in different spots, and an exponential fit is performed to the data of the squared ablated diameter as a function of the pulse energy [21]. Because of the very irregular spatial shape of the ablated holes generated in our samples, we determined the ablation threshold energy (E_{th}) by measuring the ablated area of the crater (A) as a function of the incident pulse energy, E_{in}. A similar regression technique was already compared with the diameter-regression technique, and the results are in agreement with the former regression method [22]. The obtained values are presented in the inset of Figure 1B. We can observe in Figure 1A a clear dependence of the ablated surface area on the energy and pulse number.

From this data, we are able to plot the threshold energy as a function of the number of applied pulses (Figure 2).

One obtains values from 0.11 to 0.06 mJ, as we increase the pulse number from 10 to 2000, respectively. Those values correspond rather well to the ablation thresholds previously reported for chalcogenide glasses [9, 23]. The ablation threshold fluence drops dramatically for $N \leq 100$, and it becomes constant as the pulse number increases ($N \geq 500$). We can observe that the ablation threshold fluence decreases with the number of applied laser pulses per spot. (e.g. 0.06 mJ for $N = 2000$). The reduction in ablation threshold with the incident laser shot number follows an exponential defect accumulation model, in which the lowering of the ablation threshold increases the defect creation probability for the next pulse, until the defect saturation is reached, and a constant value of E_{th} for the superposition of many pulses is established [24–26]. In this exponential model, the ablation threshold for the superposition of N pulses, E_N, can be described by:

$$E_N = E_\infty + [E_1 - E_\infty]\exp[-K(N-1)] \quad (1)$$

where E_∞ is the energy threshold at an infinite number of shots, and K is the incubation factor [27]. The incubation effect occurs when for multiple overlapping pulses ('N-on-1'), increased ablation efficiency can accumulate from pulse to pulse and decrease the damage threshold energy. Although simple, this model characterises the material response for cumulative ablation: for $K < 1$, incubation effects are present; if $K = 1$, the ablation threshold does not depend on the pulse superposition, and for $K > 1$, the material becomes more resistant to ablation [28]. According to the fit (dashed curve) and to Eq. (1), the single and infinity shot ablation thresholds $E_1 = 0.06$ mJ and $E_\infty = 0.12$ mJ are derived together with the value of $K = 0.012$.

Comparing the previous work reported by Liang et al. on silica glass, the incubation factor in the As_2S_3 chalcogenide glasses is almost three times lower [29] and is assigned by the presence of cumulative thermal effects in the As_2S_3 glasses; there is a strong evidence of heat accumulation due to the low thermal conductivity (2.5 mW cm^{-1} K^{-1}) compared to the silica glasses (12.3 mW cm^{-1} K^{-1}) [30], which reduces the energy per pulse required to induce ablation. The lower limit of the periodic structure formation is probably due to heating of the sample at a temperature above the melting point, i.e. the ablation threshold cannot decrease further by increasing the pulse number.

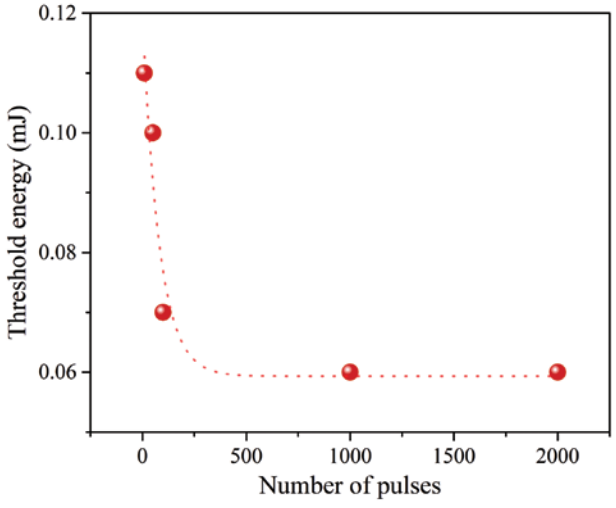

Figure 2: Threshold energy as a function of the number of applied pulses.

3.2 Laser-induced periodic surface structure formation

Several pulses ($N = 10$–2000) with energies varying from 0.1 to 2 mJ is applied on the glass surface in order to identify the parameter ranges leading to distinctive LIPSS morphologies. The formation of laser-induced periodic surface structures is observed on the ablated surface in a fluence range varying from $E = 0.1$ to 1.7 mJ and for pulse number $N < 100$ pulses. Typically, for over 100 successive pulses, periodic structures begin to disappear, perhaps by the fact that long exposures induce a heating of the sample, which

can lead to a melting of the material. In fact, for N > 100, we observe that the surface of the crater is totally smooth (not shown in the figure), and it can be attributed to the heat accumulation of subsequent laser pulses and the accompanied melting of the glass [31].

Figure 3 shows the surface morphology obtained by SEM and AFM of fs-induced periodic surface structures observed when using laser energy near the threshold energy (E = 0.1 mJ, N = 10).

We can visualise from Figure 3A a complex structuring formation showing an intermediated stage where the two periodic structures are superposed. High-spatial-frequency LIPSSs (HSFLs) with periods of 180 nm (which corresponds to $\lambda/2\eta$, where η is the refractive index of As_2S_3 glass) are found on the top of LSFL ($\Lambda \cong 720\ nm \cong \lambda$). Such ripples reaches a maximum of 200 nm in height as presented in Figure 3B and C.

Analysing carefully, we may note that the predominant direction of both types of ripples (HSFL and LSFL) coincided with the polarisation direction of the laser light. Previous works [32] have pointed out similar crests on the top of the LIPSS structures created on a krypton-doped silicon sample. The authors claim that the crests originate from a melting process, where the bubbles emerge from laser heating.

A similar surface morphology is assumed in our case on the As_2S_3 bulk glasses' surface, and the crest formation is probably due to the melting process in the centre of the ripples. Therefore, increasing the energy up to E = 0.4 mJ and keeping the pulse number constant at N = 10, we note

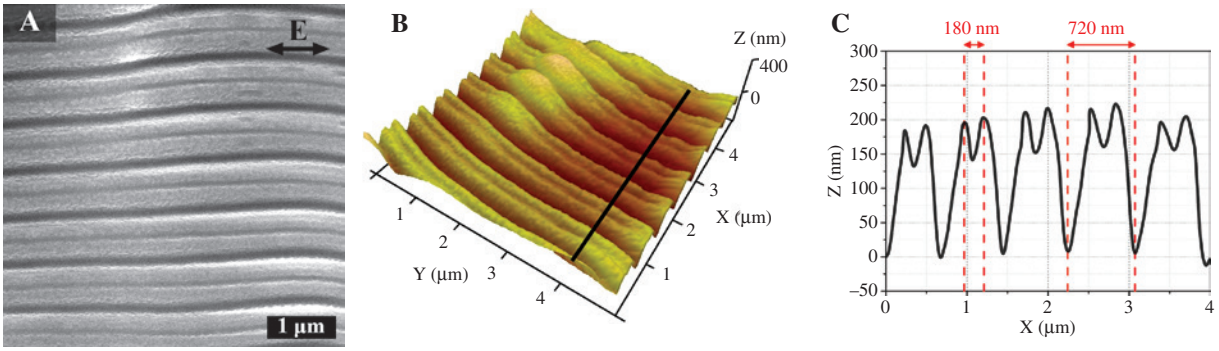

Figure 3: (A) SEM image of the surface. (B) AFM micrograph of the region irradiated by 10 subsequent laser pulses (N = 10, E = 0.1 mJ). (C) Cross-sectional profile from the black line of (B), with the different periods marked by arrows.

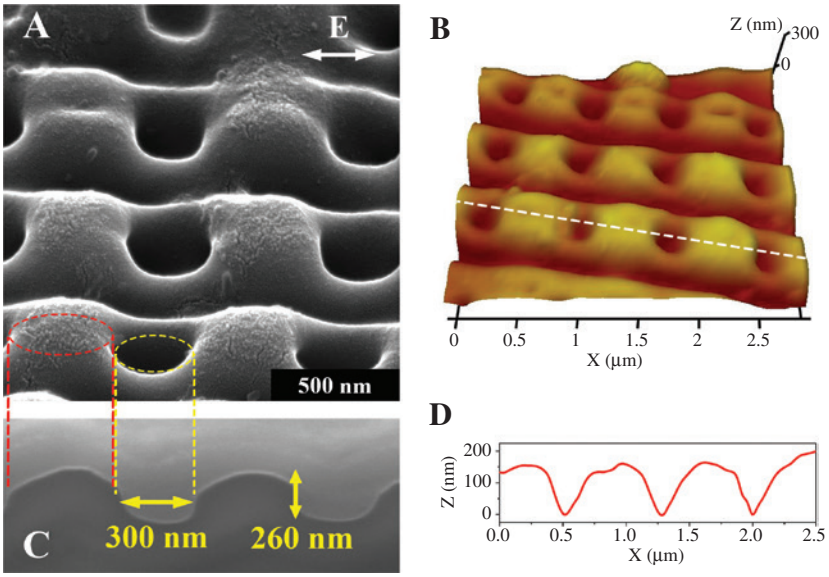

Figure 4: (A) SEM and (B) AFM images of a surface region irradiated by 10 subsequent laser pulses (N = 10, E = 0.4 mJ). (C) Corresponding SEM cross-sectional imaging, and (D) AFM cross-section corresponding to the dashed white line of (B).

the formation of periodic nanovoid structures identified through SEM micrograph and AFM image (Figure 4).

The SEM image reveals the appearance of circular nanovoids lying on the surface along the former crest obtained at 0.1 mJ (Figure 4A). Figure 4C shows the SEM cross-section image of the nanovoids produced at 0.4 mJ with an average diameter of ~300 nm and depth of 260 nm between the ripples. The picture presented in Figure 4C is performed by the deposition of Pt on the surface of the ripples and then etched down by a focused ion beam (FIB) to expose the cross section of the nanovoids. In order to map the surface microstructures, 3D AFM images of the nanovoids and cross sections of the AFM images are shown in Figure 4B, D. Similar to the SEM images, the AFM images show a periodic structure of nanovoids.

The formation of the nanovoids inside dielectrics materials has been already reported on sapphire [33] and borosilicate glass [34]. In these cases, the formation of nanovoids is achieved when the plasma generated in the focal region increases the absorption coefficient and produces a fast energy release in a very small volume. A strong shock wave is generated in the interaction region, and it propagates into the surrounding cold material. The shock wave propagation is accompanied by compression of the solid material at the wave front and decompression behind it leading to the formation of a void inside the material [35].

In our case, the formation of nanovoids in bulk chalcogenide glasses is associated with micro-explosion and can be assigned to their relatively low thermal conductivity characterised by the thermal diffusion coefficient, D, which is ~1.15×10^{-3} cm^2 s^{-1} [36] inducing an effect of temperature accumulation. Because of the increase in laser energy and/or pulse number, the temperature increases allowing a melting process of the material creating a molten layer under the expanding plasma. It means an accumulation of energy driven by a sequence of several laser pulses focused onto the same spot on the glass will occur as the period between the pulses is shorter than the cooling time. As a signature of a cumulative process, the temperature of the material drastically increases until it reaches the liquid state of the material and leads to the formation of vapour cavities in a liquid, i.e. small liquid-free zones ('bubbles' or ':voids').

When the hot liquid is ejected through the nanovoids it forms a new layer of glass from which originate the perpendicular ripples. This process leads to the formation of a new type of LIPSSs. A superposition of ripples oriented simultaneously in the direction parallel and perpendicular to the polarisation of incident light with $\Delta \cong \lambda/2\eta$ and λ resulting in structures similar to a two-dimensional grid at the target's surface as show in Figure 5 which we previously called cross-superposed LIPSSs [18].

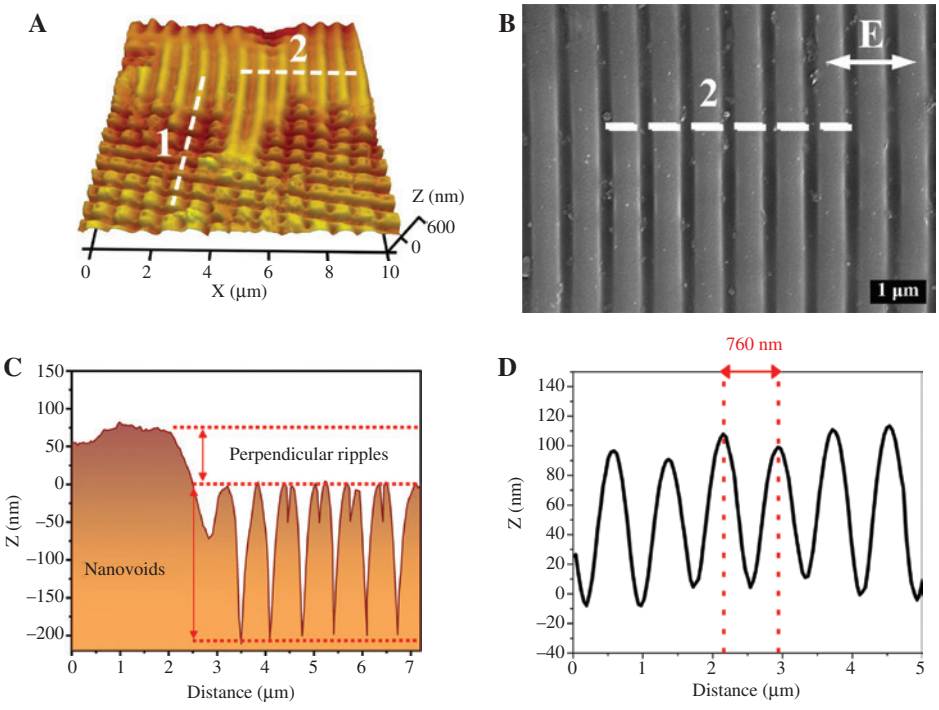

Figure 5: (A) AFM image of superposed laser-induced periodic surface structures in As_2S_3 exposed to $N<100$ successive pulses at energy below 1 mJ. (B) SEM image of ripples formed on the top of nanovoids. (C) AFM cross-section profile of dashed line 1 in (A), corresponding to the nanovoids. (D) AFM cross-section profile of dashed line 2 in (A) and (B), corresponding to the ripples.

Juodkazis et al. evoke the relationship between temperature and material ejection by exposing As_2S_3 glass to fs-laser pulses at 1-kHz repetition rate in air [37]. As a result from fs-laser pulses and As_2S_3 bulk glasses, the formation of the combined nano-fibre-spherical structures are observed. The fibres produced were of high aspect ratio, and spheres formed were embedded in the fibre with diameters up to several microns. According to the possible mechanisms proposed by the authors, the formation dynamics are determined by the interacting surface thermo-capillary (Marangoni) forces strongly coupled with thermal processes involved in jet cooling and solidification. The spherical particle formation was associated with liquid jet free energy minimisation.

AFM investigations and SEM images yield further information about the cross-superposed LIPSSs. Figure 5A shows a three-dimensional (3D) plot of the AFM data scanned over a 10 μm × 10 μm region at the intersection of the two layer structures (nanovoids and ripples). At the two regions (marked linescan 1 and linescan 2), depth profiles were extracted from the AFM data and are plotted in Figure 5C and D.

The 3D plot confirms the transition to nanovoids and surface periodic structures (Figure 5C). The difference between the measured height of the first layer composed of voids (160 nm) and the second layer composed of ripples (210 nm), which represents 50 nm, confirms the hypothesis that the perpendicular LSFL-ripples rising above the nanovoids originate from the material ejected by the micro-explosion.

Once the superposed LSFL-ripple structures are formed (typically $10 < N < 100$), the spacing between the LSFL-ripples (Figure 5B), and hence their periodicity, remains nearly constant (760 nm) as well their amplitude (100 nm) irrespective of the number of subsequent laser pulses. Above 100 successive pulses, a softening process takes place on the surface of the ablated region.

Related to the temperature influence on the periodic surface structures, it was reported [38] that irradiation of the As_2S_3 chalcogenide glass by a train of focused fs-laser pulses results in the formation of submicron structures in the bulk of the sample with modified optical properties. The authors proposed that upon two-photon absorption of laser radiation (the bandgap in As_2S_3 is $Eg = 2.55$ eV, and the energy of a laser photon is 1.55 eV), electrons from the valence band are transferred to the conduction band. During the subsequent energy relaxation in the conduction band and recombination of electrons back to the valence band, most of the energy spent on ionisation is transformed into heat.

To analyse the dependence of the ripples with laser polarisation, we change the laser polarisation to 90° with regard to the original direction. The cross-superposed ripples are rotated 90°, that is, the ripples still keep the direction perpendicular and parallel to the laser polarisation, respectively, as shown in Figure 6. It is clear that the orientation of the ripples is strongly dependent on the polarisation of incident light.

Some authors [39, 40] observed the formation of surface periodic structure ripples in thin chalcogenide glass films under exposure by polarised light at a wavelength near the bandgap. They claim that ripple formation occurs due to lateral mass transport [41] accelerated by light driven by competition between capillary forces and redistribution of electrons and holes generated by light. However, it is known that the photoinduced phenomena in As_2S_3 glasses is athermal and could not completely

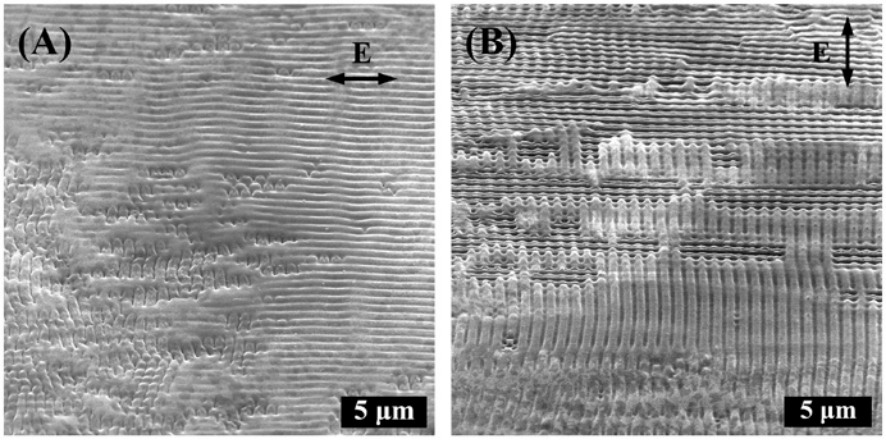

Figure 6: SEM images of the ripples depending on the laser polarisation direction: (A) horizontal, and (B) vertical. $E = 0.2$ mJ and $N = 10$, for both (A) and (B).

explain the observed cross-superposed LIPSS by models proposed for CW laser irradiation.

In the same way, it is very interesting to note at this point, that the classical model of ripple formation after fs-pulsed laser irradiation based on interference of incident laser with surface scattered waves [42] cannot fully describe the cross-superposed surface structures observed in the above results. However, the different morphologies may be an indication of different mechanisms for ripple formation, as well as different outcomes for the same mechanism. There are two mechanisms that have been discussed in the literature, which try to explain the laser-induced periodic structures induced by the fs-laser pulse: The first one is based on interference between the incident laser beam and surface plasmon-polariton waves, i.e. a purely optical approach; and the second mechanism involves hydrodynamic instabilities due to heat accumulation, which result in self-organisation effects [43]. In our case, we envisage the applicability of both these approaches, and the following mechanism of the formation of the cross-superposed LIPSSs are illustrated in Figure 7.

Figure 7A corresponds to the first stage of the formation of the HSFL ripples with a period significantly shorter than the wavelength generated by the first laser pulse. This value appears to be in agreement with the nanograting model proposed by Bhardwaj et al. in fused silica [44], where for normally incident linearly polarised light, the period Λ of the surface ripples formed due to the interference between the incident laser light, and the excited surface plasmon wave is given by:

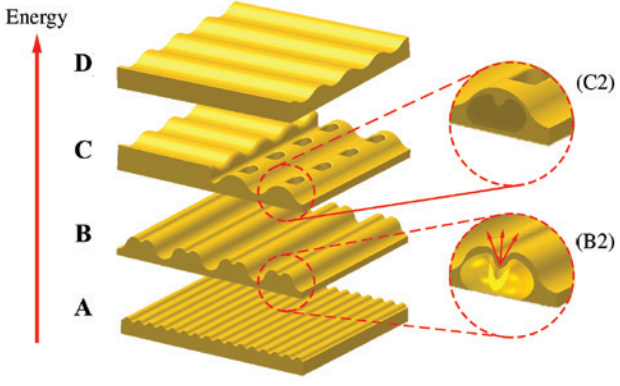

Figure 7: Schematic diagram showing the cross-superposed LIPSSs formation. The sequence of events starts with (A) LIPPSS formation by interference mechanism, due to the interference between the incident linearly polarised laser beam and the surface wave (generated by scattering during the pulse duration). (B and B2) Material was ejected from the glass surface during laser irradiation, while the glass was melted, thus, forming nanovoids and cross-superposed LIPSSs (C and C2). (D) Formation of perpendicular ripples.

$$\Lambda = \lambda/2\eta \quad (2)$$

where λ is the incident light wavelength, $\eta = \mathrm{Re}[\varepsilon/(\varepsilon+1)]1/2$ is the real part of the effective refractive index (2.4 for As_2S_3 glass) allowing only $\Lambda \leq 180$ nm as the smallest structure. According to this model, the ripple period of the As_2S_3-based glass should be constant and equal to $800/(2\times 2.4) = 166$ nm. This result implies that the Bhardwaj model can explain the ripple period properly, especially, when it is generated by the first laser pulse.

However, we assumed, due to subsequent pulses, the amount of light energy is absorbed by electrons, and the energy is transferred to the lattice [45, 46]. In this regard, the surface temperature of the As_2S_3 glass bulk sample was monitored during the exposure using a thermal camera (Jenoptik, Variocam) with a close-up lens, which provides a spatial resolution of 50 µm. We observed that the temperature of the sample would significantly increase for such longer exposures up to the point where the glass would even melt. For example, at an energy of 0.4 mJ, the glass temperature (~310°C) is reached after $N \sim 100$ successive pulses, proving that heat accumulation in the sample occurs.

When the lattice temperature at the heating surface reaches the melting point, melting takes place leading to the formation of vapour cavities in a liquid inducing the formation of bubbles (Figure 7B). As a part of the initial energy of a pulse is absorbed, glass heats up to the state of the liquid phase (above the glass transition temperature, Tg), then, cools and solidifies. Increasing the pulse number, the bubbles begin to collapse generating an array of nanovoids on the top of the ripples (Figure 7C). With increasing laser energy, the bubbles grow in size and number resulting in ejection of the material to form the perpendicular ripples (Figure 7D). According to Romanova [47], the rate of cooling at different points of the irradiated region is different, and maximum temperature is shifted toward the source of the pulse, so we can envisage that the interference generated by the plasma of the next pulse will overlap, and cross-superposed LIPSSs appear in the centre of the ablated area. From the fact that the spatial periods of the last stage producing LSFL-ripples nearly coincides with the laser radiation wavelength ($\lambda = 800$ nm), the phenomenon can be attributed to the well-known mechanism of scattering/diffraction and subsequent local-field enhancement via interference [48, 49].

Based on the above results, we speculate that the periodic surface structures are formed not only based on interference with the incident laser wave but also combined with the effect of temperature accumulation produced by

the laser pulse, which is significantly higher than that of the ablation edge. Thus, there is interplay between light diffraction and flow/ejection of molten material that induces the formation of nanovoids and cross-superposed LIPSS.

4 Conclusion

A systematic study on the interaction of As_2S_3 bulk glasses with fs-laser is presented. By varying the pulse number and the laser energy, we have been able to identify new light-induced periodic surface structures. Such structures are mostly observed in the ablated area in this system. Depending on the number and/or energy of the laser pulses applied to the same spot, a characteristic evolution from parallel HSFL passing through nanovoids to cross-superposed LIPSS and finally perpendicular HSFL ripples was observed. Compared to other glassy systems such as oxides, phosphates or fluorides, such structure has never been observed. The existence of cross-superposed LIPSSs oriented simultaneously perpendicular and parallel to the laser polarisation in As_2S_3 chalcogenide glass is assigned to the interplay between the interference of the incident laser beam and surface plasmon-polariton waves and also due to heat accumulation, which result in self-organisation effects. Additionally, we observed that the orientation of the ripples is strongly dependent on the polarisation of the incident light. Therefore, these new exotic nanostructures are suitable for the production of some integrated optical devices in the infrared region.

Acknowledgements: This research was supported by the Natural Science and Engineering Research Council of Canada (NSERC), Canada Foundation for Innovation (CFI), Canada Excellence Research Chairs (CERC on Enabling Photonic Innovations for Information and Communication), Ministère du Développement Économique, de l'Innovation et de l'Exportation (MESIE), Fonds de Recherche du Québec – Nature et technologies (FQRNT).

Author contribution

Sandra Helena Messaddeq is the researcher responsible for the research related to the interaction of femtosecond-laser with chalcogenide glasses. Antoine Dumont is responsible for AFM and SEM characterisation. Alexandre Douaud performed the sample irradiation with femtosecond laser and set up the system. Mohammed El-Amraoui prepared the chalcogenide glass samples. Younès Messaddeq is the head of the Photonic Innovations Research group.

References

[1] B. Bureau, S. Maurugeon, F. Charpentier, J.-L. Adam, C. Boussard-Pledel, et al., Fiber Integr. Opt. 28, 65–80 (2009).
[2] S. H. Messaddeq, J. P. Bérubé, M. Bernier, L. Skripachev, R. Vallée, et al., Opt. Express 20, 2824–2831 (2012).
[3] S. H. Messaddeq, V. R. Mastelaro, M. Siu Li, M. Tabackniks, D. Lezal, et al., Appl. Surf. Sci. 205, 143–150 (2003).
[4] K. Tanaka and H. Hisakuni, J. Non-Cryst. Solids 198–200, 714–718 (1996).
[5] S. N. Yannopoulos, Phys. Rev. B 68, 064206 (2003).
[6] M. I. Kozak, V. N. Zhickarev, V. I. Fedelesh, A. M. Solomon and V. Y. Loya, Advanced Photonics 2018 OSA Technical Digest (online), paper JTu2A.26. Optical Society of America (2018). https://doi.org/10.1364/BGPPM.2018.JTu2A.26.
[7] A. Douaud, S. H. Messaddeq, O. Boily and Y. Messaddeq, Appl. Surf. Sci. 445, 1–7 (2018).
[8] J. P. Bérubé, S. H. Messaddeq, M. Bernier, L. Skripachev, Y. Messaddeq, et al., Opt. Express 22, 26103–26116 (2014).
[9] S. H. Messaddeq, R. Vallée, P. Soucy, M. Bernier, M. El-Amraoui, et al., Opt. Express 20, 29882–29889 (2012).
[10] D. C. Emmony, R. P. Howson and L. J. Willis, Appl. Phys. Lett. 23, 598–600 (1973).
[11] A. E. Siegman, J. Quantum Electron. 22, 1384–1403 (1986).
[12] Z. Guosheng, P. M. Fauchet and A. E. Siegman, Phys. Rev. B 26, 5366 (1982).
[13] J. Bonse, M. Munz and H. Sturm, J. Appl. Phys. 97, 013538 (2005).
[14] J. Bonse, A. Rosenfeld and J. Krüger, J. Appl. Phys. 106, 104910 (2009).
[15] M. Soileau, IEEE J. Quantum Electron. 20, 464–467 (1984).
[16] Y. Han, X. Zhao and S. Qu, Opt. Express 19, 19150–19155 (2011).
[17] J. Reif, F. Costache, M. Henyk and S. V. Pandelov, Appl. Surf. Sci. 197/198, 891–895 (2002).
[18] J. L. Déziel, J. Dumont, D. Gagnon, L. J. Dubé, S. H. Messaddeq, et al., J. Opt. 17, 075405 (2015).
[19] I. Mirza, N. M. Bulgakova, J. Tomáštík, V. Michálek, O. Haderka, et al., Sci. Rep. 6, 39133–39142 (2016).
[20] J. M. Liu, Opt. Lett. 7, 196–198 (1982).
[21] L. M. Machado, R. E. Samad, W. de Rossi and N. D. Vieira Junior, Opt. Expr. 20, 4114–4123 (2012).
[22] N. Sanner, O. Utéza, B. Bussiere, G. Coustillier, A. Leray, et al., Appl. Phys. A 94, 889 (2009).
[23] Q. Zhang, H. Lin, B. Jia, L. Xu and M. Gu, Opt. Express 18, 6885–6890 (2010).
[24] M. Mero, B. Clapp, J. C. Jasapara, W. Rudolph, D. Ristau, et al., Opt. Eng. 44, 051107 (2005).
[25] F. Costache, S. Eckert and J. Reif, Appl. Phys. A – Mater. Sci. Process 92, 897–902 (2008).
[26] D. Ashkenasi, M. Lorenz, R. Stoian and A. Rosenfeld, Appl. Surf. Sci. 150, 101–106 (1999).
[27] A. Rosenfeld, M. Lorenz, R. Stoian and D. Ashkenasi, Appl. Phys. A 69, S373–S376 (1999).

[28] J. Bonse, J. M. Wrobel, J. Krüger and W. Kautek, Appl. Phys. A Mater. Sci. Process. 72, 89–94 (2001).
[29] F. Liang, R. Vallee, D. Gingras and S. L. Chin, Opt. Mater. Express 1, 1244–1250 (2011).
[30] D. G. Cahill and R. O. Pohl, Phys. Rev. B Condens. Matter. 15, 4067–4073 (1987).
[31] S. Richter, S. Döring, F. Burmeister, F. Zimmermann, A. Tünnermann, et al., Opt. Express 21, 15452–15463 (2013).
[32] M. Oron and G. Sorensen, Appl. Phys. Lett. 32, 782 (1979).
[33] E. G. Gamaly, Curr. Appl. Phys. 8, 412–415 (2008).
[34] S. Kanehira, Nano Lett. 5, 1591–1595 (2005).
[35] E. G. Gamaly, A. V. Rode, B. Luther-Davies and V. T. Tikhonchuk, Phys. Plasmas 9, 949–957 (2002).
[36] E. G. Gamaly, in 'Femtosecond Laser–Matter Interactions: Theory, Experiments and Applications', (Pan Stanford Publishing, Singapore, 2011).
[37] S. Juodkazis, H. Misawa, O. A. Louchev and K. Kitamura, Nanotechnology 17, 4802–4805 (2006).
[38] A. A. Babin, A. P. Aleksandrov, A. M. Kiselev, D. I. Kulagin, V. V. Lozhkarev, et al., Quantum Electron. 31, 398–400 (2001).
[39] M. L. Trunov, P. M. Lytvyn, P. M. Nagy and O. M. Dyachyns'ka, Appl. Phys. Lett. 97, 031905-1 (2010).
[40] Y. Kaganovskii, A. M. Korsunsky and M. Rosenbluh, Mater. Lett. 183, 156–160 (2016).
[41] A. Saliminia, T. V. Galstian and A. Villeneuve, Phys. Rev. Lett. 85, 4112–4115 (2000).
[42] M. Birnbaum, J. Appl. Phys. 36, 3688–3689 (1965).
[43] E. L. Gurevich and S. V. Gurevich, Appl. Surf. Sci. 302, 118–123 (2014).
[44] V. R. Bhardwaj, E. Simova, P. P. Rajeev, C. Hnatovsky, R. S. Taylor, et al., Phys. Rev. Lett. 96, 057404-4 (2006).
[45] M. Sakakura and M. Terazima, Phys. Rev. B 71, 024113 (2005).
[46] M. Sakakura and M. Terazima, Opt. Express 15(25) 16800–16807 (2007).
[47] E. Romanova, A. Konyukhov, S. Muraviov and A. Adrianov, in '12th International Conference on Transparent Optical Networks (ICTON)', IEEE, 1–4 (2010). doi: 10.1109/ICTON.2010.5549182.
[48] J. E. Sipe, J. F. Young, J. S. Preston and H. M. van Driel, Phys. Rev. B 27, 1141–1154 (1983).
[49] J. Bonse, A. Rosenfeld and J. Kruger, Appl. Surf. Sci. 257, 5420–5423 (2011).

Sandra Helena Messaddeq
Centre d'Optique, Photonique et Laser (COPL), Université Laval, Québec, Canada, e-mail: sandra.messaddeq@copl.ulaval.ca.

Dr. Sandra Helena Messaddeq is a senior scientist at COPL-Laval University (Canada) since 2010. She obtained her Ph.D. in Materials Science Engineering from the Sao Paulo State (Brazil) in 2000. Her research is focused on amorphous materials (thin film, glasses and sol-gel) and their interactions with laser irradiation to produce photonic devices and multifunctional materials including optical memory devices, 3D transparent projection screens and IR microlens arrays. She is devoted to understand their structural physical changes using Raman spectroscopy.

Antoine Dumont
Centre d'Optique, Photonique et Laser (COPL), Université Laval, Québec, Canada

Antoine Dumont is currently a doctorate student in the group of Professor Zheng-Hong Lu at the University of Toronto, working on organic light-emitting diodes and perovskite quantum dots. He received his M.Sc. degree in Physics in 2016 from York University, supported by NSERC and OGS scholarships. He also teaches Physics to students preparing for the MCAT with the company The Princeton Review.

Alexandre Douaud
Centre d'Optique, Photonique et Laser (COPL), Université Laval, Québec, Canada. http://orcid.org/0000-0002-7642-8404

Alexandre Douaud is presently working on his Ph.D. in the group of Pr. Younès Messaddeq at the Centre d'Optique, Photonique et Laser, at Université Laval (Québec, Canada). His work focuses on the phenomena that emerge from the interaction of laser with chalcogenide glasses (thin films). He previously received his Master's degree in Chemistry at Université de Rennes (France) in 2014.

Mohammed El-Amraoui
Centre d'Optique, Photonique et Laser (COPL), Université Laval, Québec, Canada

Dr. Mohammed El-Amraoui received his Master's degree in Chemistry and Physical Chemistry of Materials at Université de Montpellier (France) in 2007, and his Ph.D. in Physics at Université de Bourgogne, 2010. He is a Research Scientist at Centre d'Optique, Photonique et Laser (COPL) of Université Laval since 2011. His research interests include chalcogenide optical fibres with very low attenuation for lasers in the 3- to 5- and 8- to 14-μm windows, development of MOFs with controllable dispersion and development of compact supercontinuum sources based on chalcogenide and tellurite MOFs.

Younès Messaddeq
Centre d'Optique, Photonique et Laser (COPL), Université Laval, Québec, Canada

Younès Messaddeq holds the Canadian Excellence Research Chair in Photonic Innovations since 2010 at the Center for Optics, Photonics and Laser, at Université Laval (Quebec City). He is currently a Full Professor at the Department of Physics, Physics Engineering and Optics at Université Laval. He is also the director of the Joint International Research Unit Quebec-Brazil Photonics in collaboration with the University of Sao Paulo State (UNESP, Brazil); the director of the Laboratoire International Associé LUMAQ (Lumière Matière France Quebec) in collaboration with the Université de Bordeaux and the CNRS in France, the INRS and Université Laval in Canada; and the director of the Sentinel North Technological Platform at Université Laval since 2016. Before joining Université Laval, he was a professor and research group leader at the Institute of Chemistry of Araraquara (UNESP, Brazil), visiting professor at the IFSC, Brazil, and at the University of Münster, Germany. He has also served as a visiting researcher and fellow at the NIRIM in Japan. He has published over 450 scientific papers and has filed 33 patents.